



Contents lists available at ScienceDirect

Acta Biomaterialia

journal homepage: [www.elsevier.com/locate/actabiomat](http://www.elsevier.com/locate/actabiomat)

Full length article

## Unusual behaviour induced by phase separation in hydrogel microspheres

Clare L. Heaysman<sup>a,b</sup>, Gary J. Philips<sup>a</sup>, Andrew W. Lloyd<sup>a</sup>, Andrew L. Lewis<sup>b,\*</sup><sup>a</sup> School of Pharmacy and Biomolecular Sciences, University of Brighton, Moulsecomb, Brighton BN2 4GJ, UK<sup>b</sup> Biocompatibles UK Ltd, Farnham Business Park, Weydon Lane, Farnham, Surrey GU9 8QL, UK

## ARTICLE INFO

## Article history:

Received 29 September 2016

Received in revised form 1 February 2017

Accepted 8 February 2017

Available online xxxxx

## Keywords:

Hydrogel microspheres

Ion-exchange

Phase-separation

## ABSTRACT

Hydrogel microspheres with the capability to interact with charged species such as various drugs by ion-exchange processes are useful in a variety of biomedical applications. Such systems have been developed to allow active loading of the microsphere with chemotherapeutic agents in the hospital pharmacy for subsequent locoregional therapy of tumours in the liver by drug-eluting bead chemoembolization (DEB-TACE). A variety of microspherical embolisation systems have been described, all based upon hydrogels bearing anionic functionalities to allow interaction with cationically charged drugs. We have recently prepared a series of microspheres bearing cationic functionality and have observed some unusual behaviour induced by phase-separation that occurs during the synthesis of the microspheres. The phase-separation results in the core of the microsphere being enriched in cationic polymer component compared to the outer polyvinyl alcohol (PVA)-based phase. For certain formulations, subsequent swelling in water results in the PVA-rich skins separating from the charged cores. Ion-exchange interactions with model compounds bearing multi-anionic groups create differential contraction of the charged core relative to the skin, resulting in an unusual “golf-ball” appearance to the surface of the microspheres.

## Statement of Significance

The authors believe that the unusual behaviour of the microspheres reported in this paper is the first observation of its kind resulting from phase-separation during synthesis. This could have novel applications in drug delivery for systems that can respond by shedding their skin or altering the surface area to volume ratio upon loading a drug.

© 2017 Acta Materialia Inc. Published by Elsevier Ltd. This is an open access article under the CC BY license (<http://creativecommons.org/licenses/by/4.0/>).

## 1. Introduction

Hydrogel microspheres have a wide range of potential applications for the controlled release of pharmaceuticals and agrochemicals [1–5]. The incorporation of ionic functional groups within the polymer matrix provides an opportunity to bind cationic or anionic molecules through ion-exchange processes [6,7]. Our previous work has focussed on the synthesis of anionic hydrogel microspheres for the delivery of doxorubicin for chemoembolization therapy of malignant liver tumours [8–11]. This provides for a system which can be actively loaded with certain chemotherapeutic agents in the hospital pharmacy and subsequently provided to the interventional oncologist for administration using minimally-invasive image-guided into the arteries feeding the tumour

[12,13]. Drug is then eluted over time at the site of the tumour in a sustained and controlled fashion, with a subsequent reduction in drug-related systemic side effects [14,15]. In this case, ionic interaction is achieved by the incorporation of groups bearing sulfonic acid functionality, which interact with the protonated primary amine group of the doxorubicin hydrochloride salt, a process that can be monitored spectroscopically [12] or with calorimetry [16]. Similar effects can be achieved using other anionic functional groups such as carboxylate-bearing residues, although the strength and potential permanency of the interaction will be different [17,18].

Much of the research undertaken to date has involved the use of drugs bearing a single cationic group, although there has been some limited investigation of the use of mitoxantrone, an anthracenedione bearing two pendent cationic amine groups, which was shown to interact strongly with the anionic residues, essentially cross-linking the polymer chains and causing a severe

\* Corresponding author.

E-mail address: [andrew.lewis@biocompatibles.com](mailto:andrew.lewis@biocompatibles.com) (A.L. Lewis).

shrinkage of the microsphere diameter and concomitant increase in its compressive modulus [19–21]. Recently we described the synthesis and characterisation of a range of cationic microspheres with different loading capacities for use in the delivery of anionic drugs for a variety of drug delivery applications [22]. These were made using in a similar suspension polymerisation process to that used for the anionically-charged microspheres, involving the copolymerisation of a poly vinyl alcohol macromer bearing acrylamide-functionalities on the backbone, with (3-acrylamido propyl)trimethylammonium chloride (APTA) [10]. During the course of this investigation we noticed that some of the formulations that possessed high proportions of the APTA exhibited unusual behaviours. Herein we report the discovery of a novel hydrogel microsphere with the potential to shed its outside layer on hydration in water or to increase its surface area to volume ratio by forming a golf ball-like microsphere on hydration in solutions containing multi-anionic species.

## 2. Materials and methods

### 2.1. Materials

Poly(vinyl alcohol) (PVA) partly saponified, 88% hydrolysed, 12% acetate content, average molecular weight of 67,000 Da (trade name Mowiol 8-88, IMCD UK Ltd, Surrey, UK.), (3-acrylamidopropyl)trimethylammonium chloride (APTA) (75% w/w, Sigma-Aldrich, Poole, UK) and N-acryloyl-aminoacetaldehyde dimethyl acetal (NAAADA, Biocure, Norcross, USA) were used as received. Cellulose acetate butyrate (CAB) (Safic Alcan UK Ltd, Warrington UK) was used as a 10% solution in ethyl acetate. Pyrene sulfonic acid based sodium salts were supplied by Sigma Aldrich, UK. Water was purified by reverse osmosis using a Millipore (UK) Ltd Elxi 10 water purification system. Sodium chloride was supplied by Fisher Scientific UK. Phosphate buffered serology saline (PBS) was supplied by Inverclyde Biologicals, UK. Solvents were supplied by Romil Ltd. UK and all other materials were supplied by Sigma-Aldrich, UK and were used as received.

### 2.2. Microsphere synthesis

The process for the synthesis of APTA-modified PVA microspheres has been described in detail by us elsewhere [22]. In brief, PVA was functionalised with NAAADA by an acid-catalysed reaction in aqueous solution, to form cyclic acetal linkages with the macromer. Insoluble microspheres were produced by a water-in-oil suspension polymerisation in which the macromer was copolymerised with APTA by redox-initiated polymerisation using ammonium persulfate (APS) in the aqueous phase and tetramethylethylenediamine (TMEDA) in the oil phase. Beads were produced in various sizes, typically 100 to 1500  $\mu\text{m}$ . The proposed reaction scheme is presented in Fig. 1.

Seven different formulations (APTA<sub>0</sub>, APTA<sub>16</sub>, APTA<sub>27</sub>, APTA<sub>43</sub>, APTA<sub>60</sub>, APTA<sub>86</sub> and APTA<sub>100</sub>) were prepared by increasing the weight percentage (wt%) of APTA in the aqueous phase and keeping the total amount of water, macromer and APS the same [22]. Notation for the formulations represents the ratio of weight percentage (wt%) for APTA to macromer used in synthesis e.g. APTA<sub>60</sub> denotes 60 wt% APTA: 40 wt% macromer. APTA<sub>0</sub> are microspheres composed of solely the cross-linked PVA macromer and APTA<sub>100</sub> was prepared using just APTA alone and an additional non-ionic acrylamide monomer (N,N'-methylenebisacrylamide) in order to cross-link the microspheres.

### 2.3. Image analysis

Optical microscopy imaging was performed using an Olympus BX50F4 microscope. Images were captured with a ColorView III (Olympus, Japan) high resolution digital camera attached to the microscope. Microsphere sizing was performed manually using the sizing tool of AnalySIS software (Soft Imaging System GmbH). Environmental scanning electron microscopy imaging was performed on microspheres previously washed in water and then placed on a metallic stub and imaged using low vacuum JEOL Scanning Electron Microscope, JCM 5700, 100 Pa, BES 20 kV.

### 2.4. Attenuated total reflectance fourier transform infrared spectroscopy (ATR-FTIR)

A PerkinElmer Spectrum One FTIR Spectrometer with Universal Attenuated Total Reflectance (UATR) accessory and diamond crystal was used in the analysis of samples. A selection of microspheres of each formulation were dehydrated in acetone and then dried under vacuum at 120 °C. The microspheres were ground into a powder using a pestle and mortar before final drying to a constant weight. Each sample was scanned 4 times and subjected to baseline correction. In the interpretation of the spectra bands, identification was performed with reference to group frequency tables published in available literature [23–26].

### 2.5. Loading of model drugs into cationic microspheres

The model drugs used in this study were dyes based on pyrene with varying degrees of substitution with sulfonic acid groups: 1-pyrenesulfonic acid sodium salt (P1), 6,8-dihydroxypyrene-1,3-disulfonic acid disodium salt (P2), 8-hydroxypyrene-1,3,6-trisulfonic acid trisodium salt (P3) and 1,3,6,8-pyrenetetrasulfonic acid hydrate tetrasodium salt (P4). The dyes were all dissolved in deionised water before addition to a slurry of microspheres. The loading method was as described previously [22]. To achieve the maximum loading capacity each microsphere formulation was loaded using approximately 5 mg of excess dye per mL of microspheres, based on the calculated theoretical capacities (assuming a 1:1 sulfonic acid: APTA binding ratio). For the duration of loading (72 h) the vial was rolled to mix at room temperature. After loading the microspheres were repeatedly washed with deionised water to remove residual unbound dye. Loading was monitored by removing aliquots of the loading solution which were analysed by visible spectroscopy. The maximum binding capacity of each formulation with each dye was determined by extraction for 7 h in an ionic solution (500 mL of a saturated KCl solution in water, mixed to a 50:50 ratio with ethanol).

### 2.6. Confocal Laser Scanning microscopy (CLSM)

Microspheres loaded with dye to maximum binding capacity, stored in water, were imaged using a Leica TCS SP5 confocal, with a Leica DMI6000 B inverted microscope and HCPL Fluotar x20 0.5 dry objective lens.

## 3. Results and discussion

### 3.1. Microsphere composition and appearance

The incorporation of APTA for all microsphere formulations was confirmed by CHN analysis and image analysis demonstrated that uniformly spherical microspheres were produced using the same synthetic process [22]. For use in chemoembolization therapy hydrogel microspheres are provided in narrower size ranges

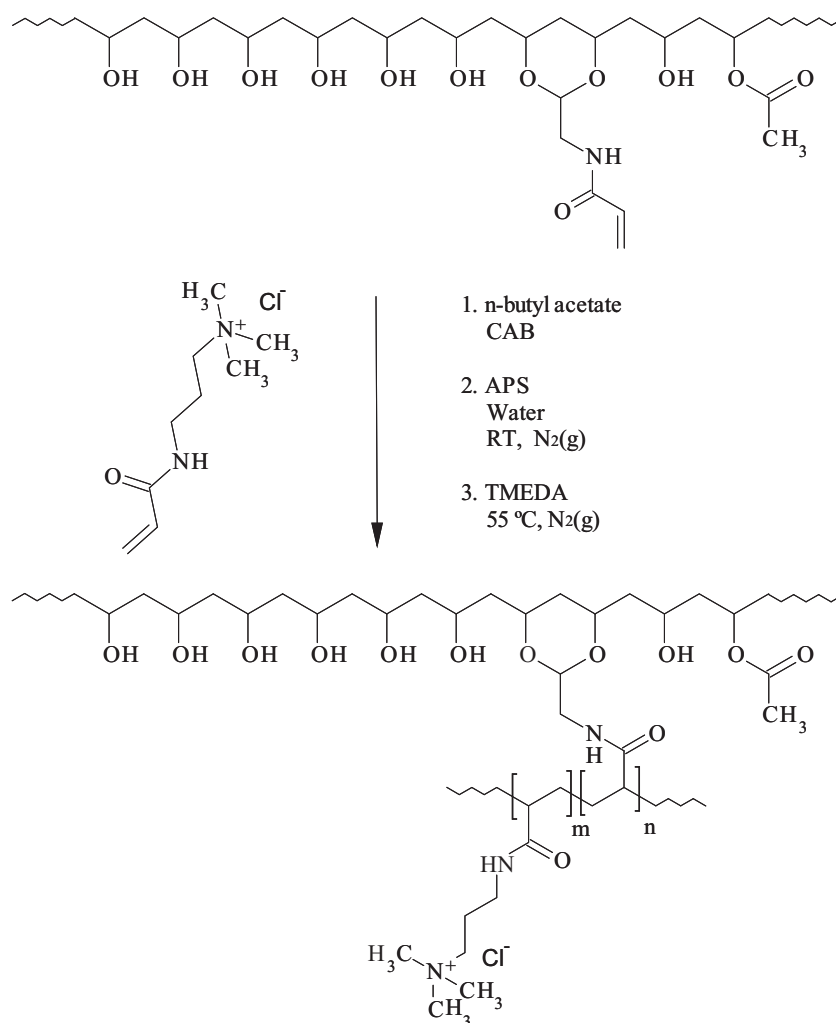


**Fig. 1.** Proposed reaction scheme for the synthesis of cationic microspheres. The end product is a simplified representation of the polymer structure where  $n$  is fixed in the preparation of the macromer and  $m$  is varied in each formulation.

achieved by sieving the bulk 100 to 1500  $\mu\text{m}$  sizes into different fractions. The microspheres described here were also separated into different fractions using sieves. In Fig. 2 optical images of APTA<sub>16</sub> to APTA<sub>60</sub> microspheres, collected from the 710 to 900  $\mu\text{m}$  sieved fractions, show that these microspheres are not damaged following sieving. Fig. 2 also illustrates that for larger microsphere sizes than previously presented, APTA<sub>60</sub> microspheres still appear visibly more opaque than the other formulations. In our initial study we suggested that the opacity of APTA<sub>60</sub> microspheres may be indicative of phase separation between the cationic acrylamide and PVA macromer when higher concentrations of the cationic acrylamide are used in the formulation. [22].

The possibility of phase separation in formulations with high concentrations of APTA was also apparent in image analysis of APTA<sub>86</sub> microspheres [22]. In our initial study we observed that although several APTA<sub>86</sub> microspheres appeared spherical there were also many with possible surface deformities. On closer inspection these microspheres appeared to have an inner core surrounded by an outer skin. The skin was often pictured as peeling away from the core or as loose structures in the solution (Fig. 3 (a)). Fig. 3(b) shows this in more detail under environmental SEM where the skin has peeled away to reveal an inner core that has slightly dehydrated under the SEM vacuum, suggesting higher water content than the skin material.

### 3.2. Spectroscopic analysis of the phase-separated components

Fig. 4 shows the comparison of the FTIR spectra for Mowiol 8-88 PVA, APTA<sub>0</sub> and APTA<sub>100</sub> formulations. Alcohols commonly have broad absorption bands between 3700 and 3580  $\text{cm}^{-1}$ . However, in polymer structures where hydrogen bonding can exist between hydroxyl groups, the force constant of the bonds can alter and O–H stretching bands move to lower frequencies. In these PVA based materials the broad band at approximately 3327  $\text{cm}^{-1}$  can be attributed to hydrogen bonded O–H groups whereas absorption bands near 2910  $\text{cm}^{-1}$  are caused by C–H stretching of the polymer backbone. In Mowiol 8-88 PVA the intense peak at 1733  $\text{cm}^{-1}$  is caused by stretching of C=O of the acetate groups. APTA<sub>0</sub> microspheres are formed through the polymerisation of the PVA macromer only and it was assumed that 100% hydrolysis of acetate groups along the backbone occurs during synthesis and heat extraction of the beads. This is confirmed by the absence of a peak at 1730  $\text{cm}^{-1}$ . Note that there is a unique band at 842–846  $\text{cm}^{-1}$  for the PVA-based compositions that is absent in the APTA only formulations. In the formation of macromer, PVA is functionalised with NAAADA. Amides have distinctive vibrational bands corresponding to N–H and C=O stretching. N–H stretching of amides occurs at 3330–3060  $\text{cm}^{-1}$  for solid samples. Therefore, in these microsphere structures the broad peak at 3295  $\text{cm}^{-1}$  can be assigned to the combination of O–H and N–H stretching. Carbonyl

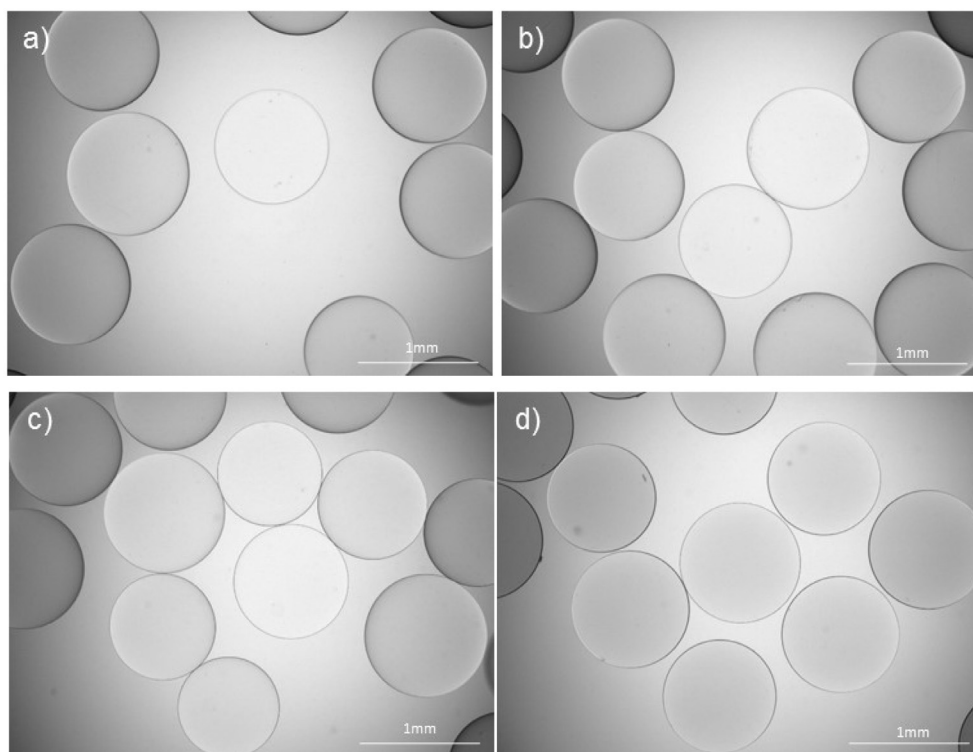


**Fig. 2.** Optical images of microspheres in saline a) APTA<sub>16</sub>, b) APTA<sub>27</sub>, c) APTA<sub>43</sub> and d) APTA<sub>60</sub>.

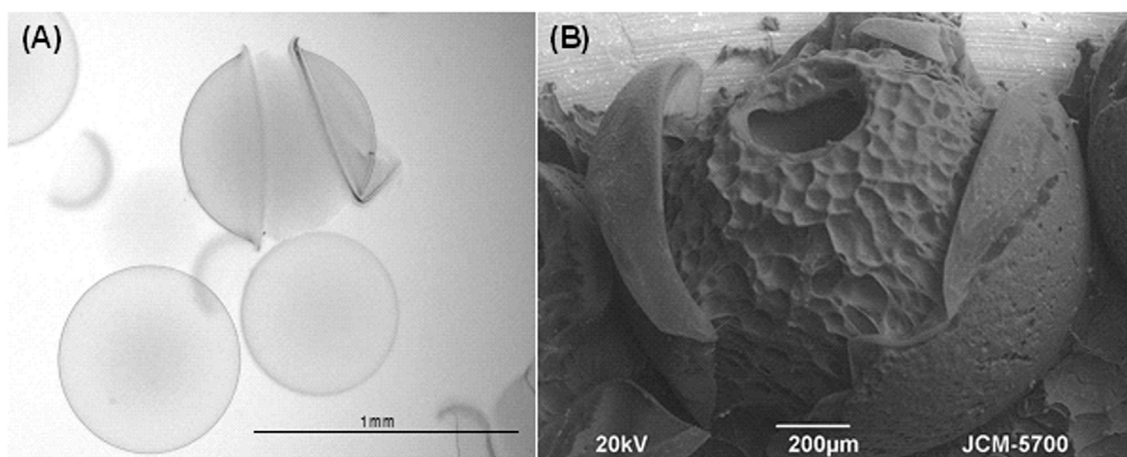


**Fig. 3.** (A) Optical image of APTA<sub>86</sub> beads where one bead has a 'core and skin' like appearance; (B) Environmental SEM image of single APTA<sub>86</sub> bead in which the skin has peeled away to reveal an inner core that is partially dehydrated by the imaging method.

groups exhibit strong absorption bands between 1870 and 1540  $\text{cm}^{-1}$ . The position of the C=O stretching band is determined by factors such as hydrogen bonding, neighbouring groups and the physical state of the compound. In amides the carbonyl absorbance bands (amide I band) are at a lower frequency than that of the acetate group due to the effect of resonance which effectively increases the C=O bond length.

Although the initial elemental analysis of APTA<sub>86</sub> microspheres determined that they have the same composition as predicted theoretically [22], it was possible to separate the skins from the stable cores by additional sieving, and after dehydration they were tested separately by ATR-FTIR and elemental analysis. The average results of elemental analysis for the separated cores and skins showed

similar C and H values but significant differences in N content (Cores vs Skins: C = 50.6% vs 49.6%; H = 9.6% vs 9.5%; N = 11.0 vs 6.0). This variation suggests that the cores and skins have a different composition. Based on these values, the elemental composition of the skins was calculated to be approximately 71% macromer to 29% APTA and the cores 21% macromer to 79% APTA indicating that the cores are predominately APTA. This result is corroborated by comparison of the respective ATR-FTIR spectra shown in Fig. 5. Although there are common peak positions, the cores of APTA<sub>86</sub> have an absence of the strong peak at 845  $\text{cm}^{-1}$  assigned to C-C stretching of the PVA backbone [23]. This band is also absent from APTA<sub>100</sub> microspheres which have no macromer in their formulation (Fig. 5) which confirms that less macromer is present.

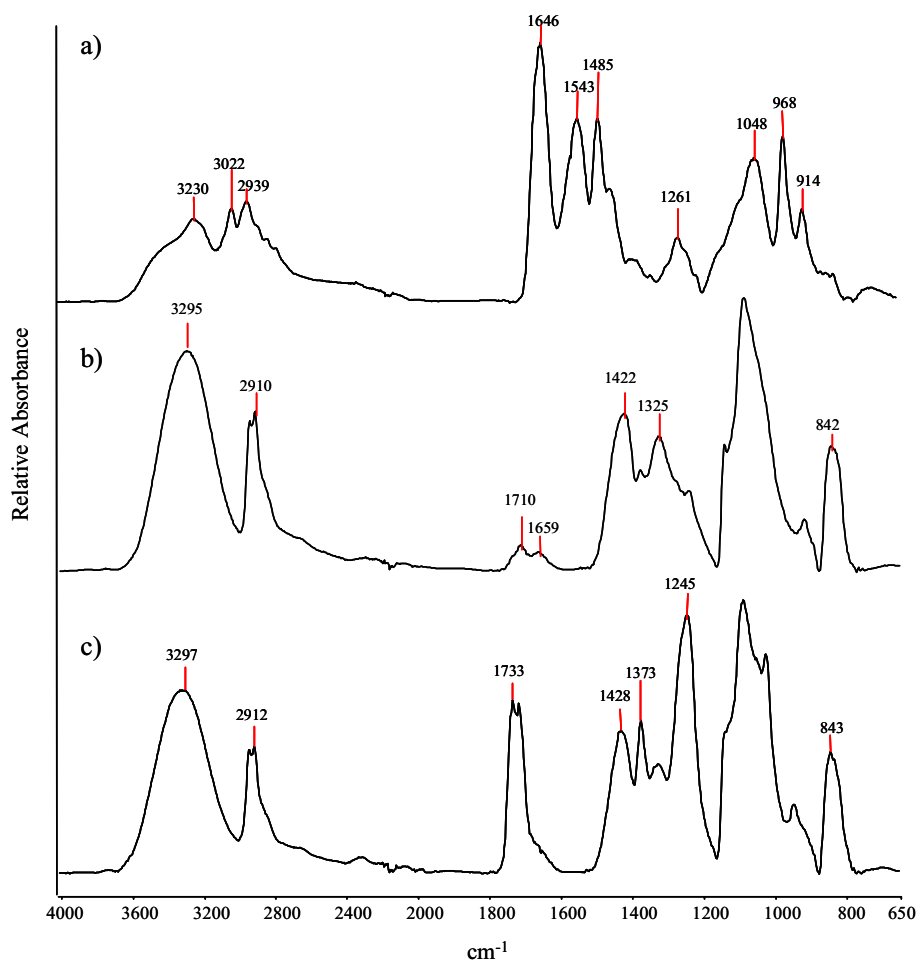


Fig. 4. ATR-FTIR spectra of a) APTA<sub>100</sub>, b) APTA<sub>0</sub>, c) Mowiol 8-88 PVA.

### 3.3. Microsphere interaction with model anionically-charged compounds

Ion-exchange microspheres uptake ionic compounds and retain them in their matrix. There is no diffusion of the compound into solution unless a counter ion is present. Cationic microspheres can be clearly imaged when loaded with the coloured pyrene sulfonic acid based sodium salts using both optical and confocal microscopy techniques. Previous analysis of loaded cationic microspheres using optical microscopy has demonstrated that when more dye is loaded the microspheres can appear darker and have a different colour [22]. The APTA<sub>60</sub> formulation when loaded to maximum capacity with pyrene dyes appear brown to black (Fig. 6). Careful examination of the images for the APTA<sub>60</sub> formulation reveals an intriguing surface feature on microspheres loaded with any of the model drug species (Fig. 7(a)). Also evident on this optical microscopy image is a thin clear layer at the edge of the microsphere, indicating a substantially drug-free outer skin exists. This was further investigated using a CLSM 3D reconstruction and clearly shows that these microspheres possess “golf ball”-like surface indentations, of approximately 50  $\mu\text{m}$  each in diameter and 20–30  $\mu\text{m}$  in depth (Fig. 7(b)). The fluorescence that produces this image originates from the dye loaded throughout the microsphere core region. Fig. 7(c) shows an environmental SEM image of the APTA<sub>60</sub> formulation, this time loaded with dye P4 but still resulting in a uniform dimpled surface appearance.

### 3.4. Rationale for usual microsphere behaviour

Synthesis of the microspheres is initiated using APS and TMEDA as described in Lewis et al. [10]. APS is water soluble and is dissolved in the aqueous phase of the suspension. As TMEDA is added to the organic phase radicals are generated at the surface of the droplets causing the microspheres to have a more highly cross-linked outer layer [27]. However, with greater than 86% APTA in the formulation the compatibility between the PVA macromer and acrylic monomer is reduced. This is a similar effect to that described by Demchenko et al. [28] in the study of PVA-PAA graft copolymers. PVA, although a hydrophilic polymer, is relatively hydrophobic in comparison to the cationic monomer, due to its long hydrocarbon backbone and the absence of ionic moieties in its structure. PVA is commonly used to stabilise suspension polymerisations, forming a protective film around the suspended droplets [29]. In the systems described here the macromer appears to have greater affinity for the hydrophobic organic phase and associates at the surface of droplet during polymerisation. Therefore, the high APTA concentration results in a predominately APTA-rich core with PVA macromer at the surface. When the microspheres are hydrated in water the APTA rich phase, which is more hydrophilic than the outer PVA phase, becomes more swollen splitting the outer skin. It is likely that if the outer ‘skin’ layer does not swell to the same degree it separates from the inner core (Fig. 8).

The intermediate formulations, with APTA content up to 60 wt %, therefore appear to provide a better balance of properties in

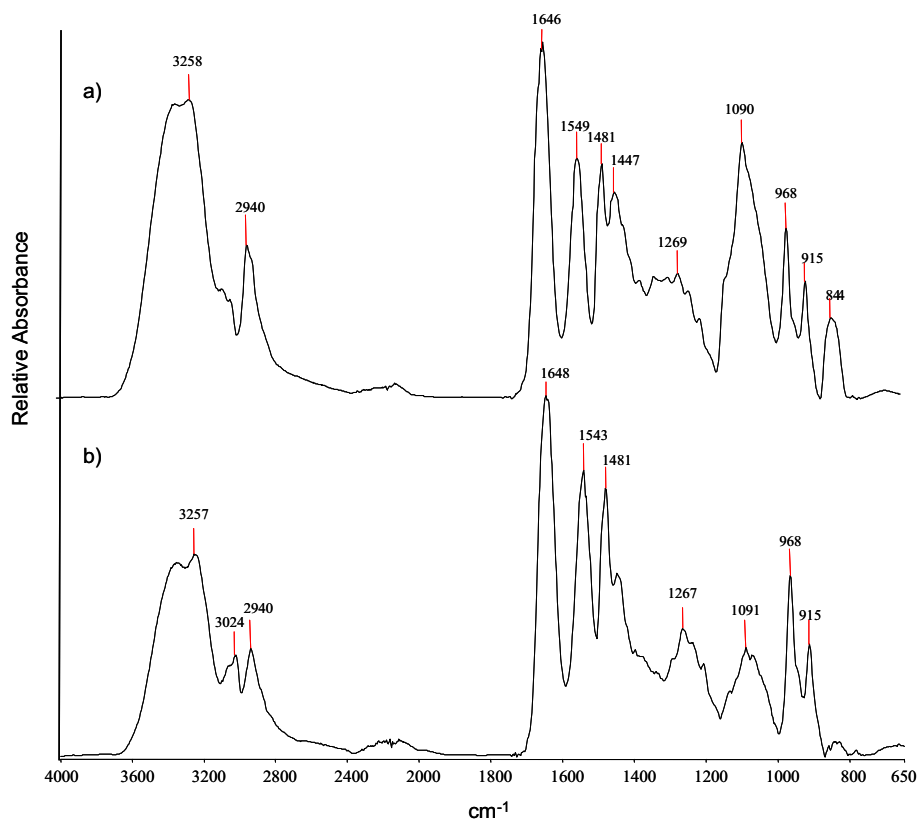


Fig. 5. ATR-FTIR spectra for APTA<sub>86</sub> a) skins b) cores.

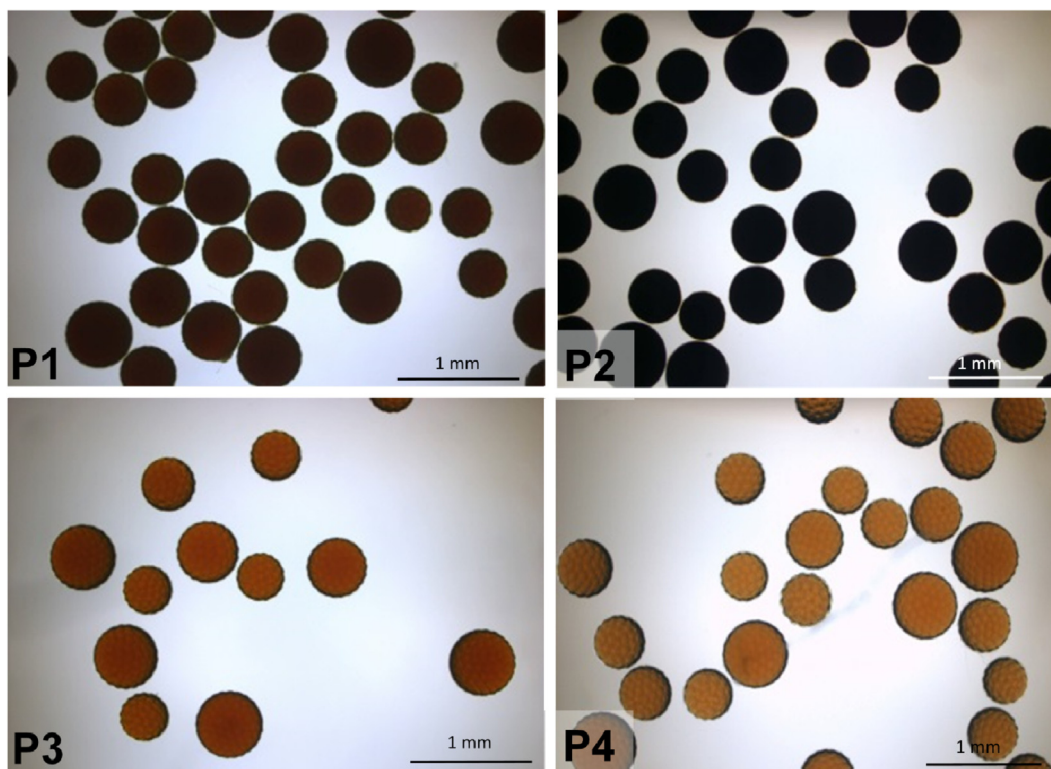
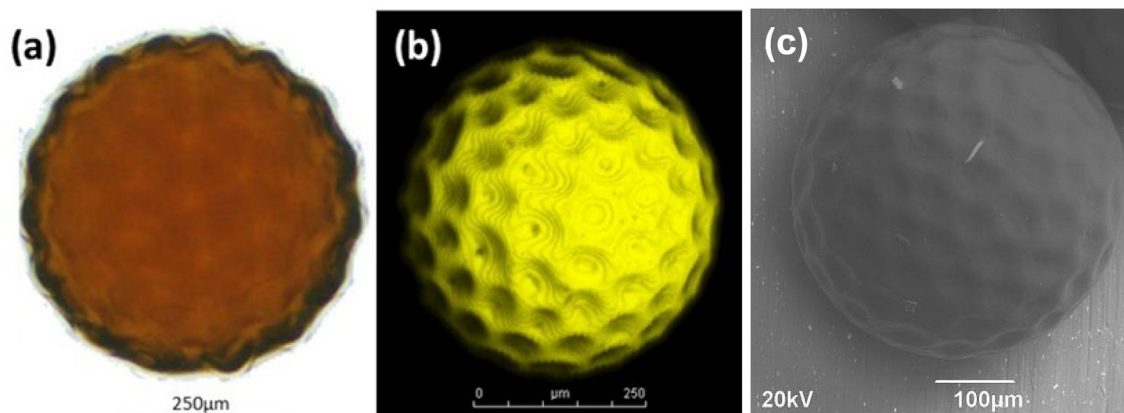
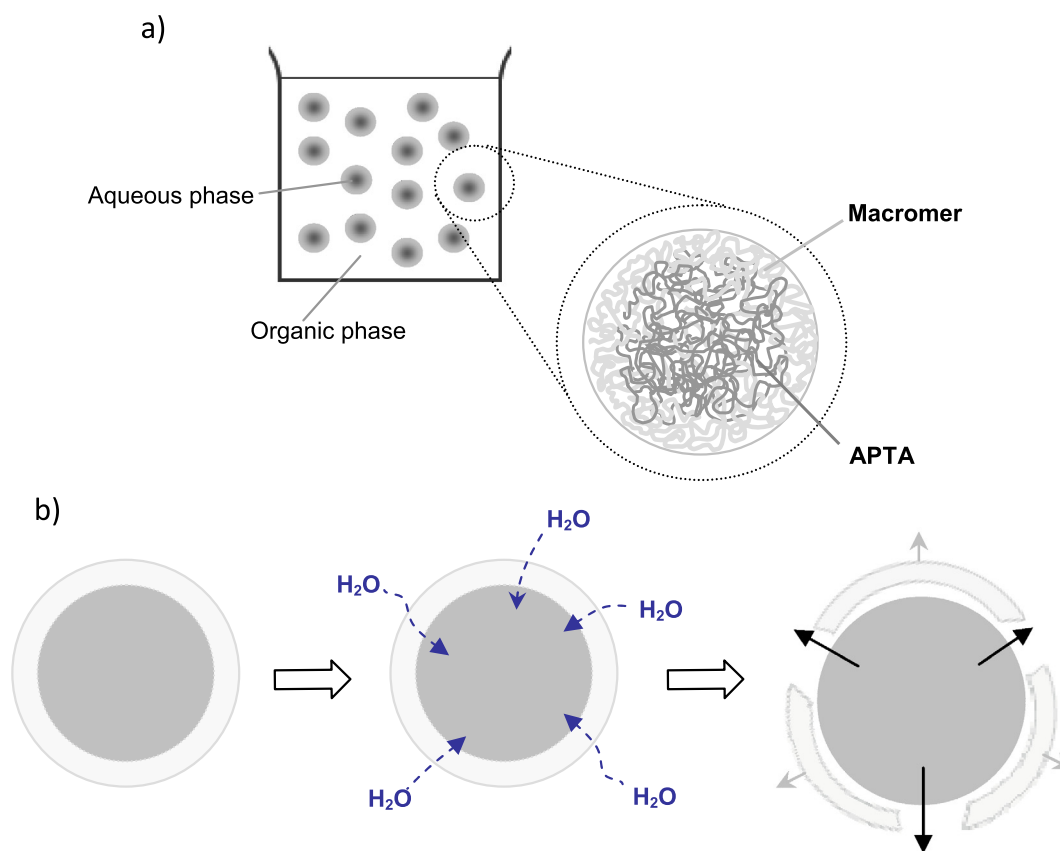


Fig. 6. Transmitted light images of APTA<sub>60</sub> cationic microspheres loaded to maximum capacity with anionic dyes P1, P2, P3 and P4.



**Fig. 7.** (a) Magnified image of APTA<sub>60</sub> loaded with P3; (b) 3D confocal projection of APTA<sub>60</sub> microspheres loaded to maximum capacity with P3; (c) Environmental SEM image of APTA<sub>60</sub> loaded with P4.



**Fig. 8.** Illustration of APTA<sub>60</sub> microspheres a) distribution of APTA formed during initiation, b) swelling of microsphere in water bursting outer skin.

terms of minimal phase separation and hence stability upon swelling e.g. good mechanical properties, sufficient number of ionic binding sites for drug interaction and high water contents to allow ease of diffusion. There are, however, fewer therapeutic agents that are salts that carry an overall negative charge compared to those with a positive charge. In a study published by Nagai and co-workers [30], the authors opted to select a number of dyes with different charge densities to model release kinetics through peptide hydrogels. In particular the study investigated the use of two pyrene sulfonic acid based sodium salts, with three or four sulfonic acid side groups. It was demonstrated that there was a reduction in diffusivity through the hydrogels with an additional sulfonic acid group that was attributed to the increase in electrostatic interac-

tion with the peptide. Henceforth, to characterise the ability of the cationic microspheres described here to act as ion-exchange systems, four different pyrene sulfonic acid based sodium salts were selected to act as model anionic drugs. It was the hypothesis that the negative sulfonic acid groups of the dyes would be able to bind to the ammonium groups of the polymer by ion-exchange. The dyes have very similar structures and their use was intended to allow easy comparison upon loading and elution. Dyes P1 to P4 have progressively more sulfonic acid groups and consequently more sites available for binding.

The model anionic drugs P2, P3 and P4 have multiple binding sites which influences their loading ability. The loading capacity of the microspheres loaded with P3 and P4 were approximately

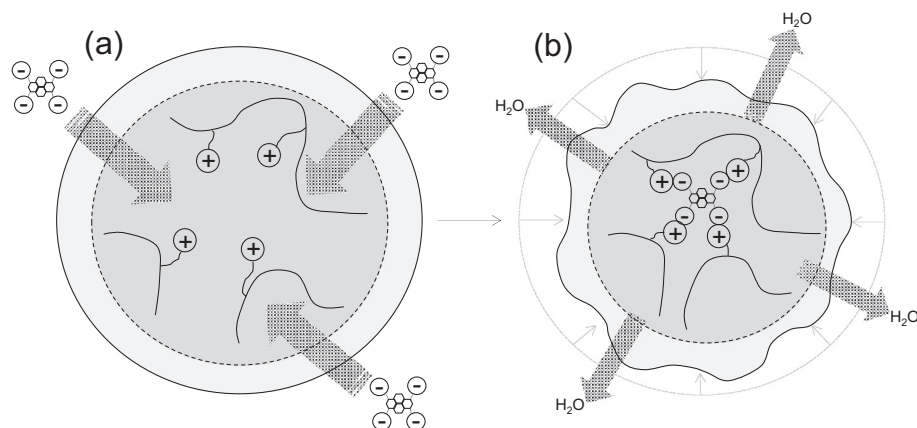


**Fig. 9.** Illustration of dye loading (a), interacting with binding sites at the APTA-rich core causing ionic cross-linking, displacing water from the interstitial spaces and a differential contraction of the core versus the skin leading to dimpled surface features (b).

30% and 25% respectively, of the theoretically available quaternary ammonium groups [19,22]. In Fig. 9 the process of loading P4, a multivalent dye is illustrated. It can be postulated that when using dyes with multiple binding sites, most of the adjacent sites are capable of binding to the molecule due to the polymer network flexibility and the maximum loading capacity is achieved.

CLSM has been used in this study to visualise the location of dye within the loaded microspheres and moreover reveal some interesting surface features not clear under optical microscopy. The 3D confocal projection of a P3 APTA<sub>60</sub> loaded microsphere reveals a very uniform surface structure, resembling a golf ball (Fig. 7). Golf ball-like structures have previously been described by other authors [31,32]. However, these structures were formed during polymerisation and not from pre-formed microspheres as seen here. APTA<sub>60</sub> microspheres have been described as highly compressible in their unloaded state and have high water contents. During loading, drug binds to the APTA groups concentrated at the centre of the spheres and the structure collapses as water is lost and the surface area is reduced. The surface layer contains less APTA and hence is less affected; the differential volume contraction of the core versus the skin therefore yields a dimpled surface resembling a golf ball. Similar observations have been made with polystyrene (PS)/poly(styrene-co-sodium styrene sulfonate) (P(S-NaSS))/poly(n-butyl methacrylate) (Pn-BMA) composite particles which are fabricated with a different seed and shell composition that undergoes volume reduction in the core domains leading to a golf ball-like appearance [33]. This interesting effect will increase the surface area to volume ratio which could be a useful feature for controlling drug elution rates. This study provide a basis for future studies to better understand the formation, surface properties and drug eluting characteristics of these unusual phase separated APTA-based “golf-ball” systems in relation to other factors such as pH and ionic strength. These systems may also offer opportunities for anchoring other particles, enhancing cell adhesion or acting as DNA carriers as described for other dimpled microspheres [34–36].

#### 4. Conclusions

We have performed more detailed investigation into the effects of increasing APTA monomer concentration in PVA copolymer microsphere synthesis. We have shown that microspheres prepared using greater than 60% APTA appear to undergo phase separation to form a microsphere structure with an inner acrylamide-rich core surrounded by an outer, predominately PVA, skin. Upon hydration the inner core appears to have a higher degree of swell-

ing and can burst open the outer skin. Ionic interaction between model anionic dyes possessing multiple charged groups per molecule and the APTA sites along the copolymer chains, effectively ionically cross-links the APTA rich core of the microspheres. This results in a differential volume contraction in the core versus the skin of the microsphere in these high APTA formulations, creating an interesting golf ball-like dimpled surface morphology which may have a range of potential applications.

#### Acknowledgements and disclosures

CLH would like to thank SEEDA for the provision of an EPSRC CASE award and Biocompatibles UK Ltd for sponsorship under which this study was performed. ALL is an employee of Biocompatibles UK Ltd which manufactures microspheres for use in embolisation therapy.

#### References

- [1] G. Cirillo, S. Hampel, U.G. Spizzirri, O.I. Parisi, N. Picci, F. Iemma, Carbon nanotubes hybrid hydrogels in drug delivery: a perspective review, *Biomed. Res. Int.* 2014 (2014) 825017.
- [2] R.V. Kulkarni, S. Biswanath, Electrically responsive smart hydrogels in drug delivery: a review, *J. Appl. Biomater. Biomech.* 5 (2007) 125–139.
- [3] S.K. Kushwaha, P. Saxena, A. Rai, Stimuli sensitive hydrogels for ophthalmic drug delivery: a review, *Int. J. Pharm. Invest.* 2 (2012) 54–60.
- [4] G. Tripodo, G. Pitarresi, F.S. Palumbo, E.F. Craparo, G. Giammona, UV-photocrosslinking of inulin derivatives to produce hydrogels for drug delivery application, *Macromol. Biosci.* 5 (2005) 1074–1084.
- [5] A.R. Kulkarni, K.S. Soppimath, T.M. Aminabhavi, A.M. Dave, M.H. Mehta, Glutaraldehyde crosslinked sodium alginate beads containing liquid pesticide for soil application, *J. Control. Release* 63 (2000) 97–105.
- [6] A. Piesz, M.K. Bak, Raman spectroscopy and WAXS method as a tool for analysing ion-exchange properties of alginate hydrogels, *Int. J. Biol. Macromol.* 43 (2008) 438–443.
- [7] F. Horkay, I. Tasaki, P.J. Bassar, Effect of monovalent-divalent cation exchange on the swelling of polyacrylate hydrogels in physiological salt solutions, *Biomacromolecules* 2 (2001) 195–199.
- [8] R.E. Forster, S.A. Small, Y. Tang, C.L. Heaysman, A.W. Lloyd, W. Macfarlane, G.J. Phillips, M.D. Antonijevic, A.L. Lewis, Comparison of DC Bead-irinotecan and DC Bead-topotecan drug eluting beads for use in locoregional drug delivery to treat pancreatic cancer, *J. Mater. Sci. – Mater. Med.* 21 (2010) 2683–2690.
- [9] M.V. Gonzalez, Y. Tang, G.J. Phillips, A.W. Lloyd, B. Hall, P.W. Stratford, A.L. Lewis, Doxorubicin eluting beads-2: methods for evaluating drug elution and in-vitro:in-vivo correlation, *J. Mater. Sci. – Mater. Med.* 19 (2008) 767–775.
- [10] A.L. Lewis, M.V. Gonzalez, S.W. Leppard, J.E. Brown, P.W. Stratford, G.J. Phillips, A.W. Lloyd, Doxorubicin eluting beads – 1: effects of drug loading on bead characteristics and drug distribution, *J. Mater. Sci. – Mater. Med.* 18 (2007) 1691–1699.
- [11] A.L. Lewis, M.V. Gonzalez, A.W. Lloyd, B. Hall, Y. Tang, S.L. Willis, S.W. Leppard, L.C. Wolfended, R.R. Palmer, P.W. Stratford, DC Bead: in vitro characterization of a drug-delivery device for transarterial chemoembolization, *J. Vasc. Interv. Radiol.* 17 (2006) 335–342.

- [12] A.L. Lewis, M.R. Dreher, Locoregional drug delivery using image-guided intra-arterial drug eluting bead therapy, *J. Control. Release* (2012).
- [13] A.L. Lewis, R.R. Holden, DC Bead embolic drug-eluting bead: clinical application in the locoregional treatment of tumours, *Expert Opin. Drug Deliv.* 8 (2011) 153–169.
- [14] J. Lammer, K. Malagari, T. Vogl, F. Pilleul, A. Denys, A. Watkinson, M. Pitton, G. Sergent, T. Pfammatter, S. Terraz, Y. Benhamou, Y. Avajon, T. Gruenberger, M. Pomoni, H. Langenberger, M. Schuchmann, J. Dumortier, C. Mueller, P. Chevallier, R. Lencioni, Prospective randomized study of doxorubicin-eluting-bead embolization in the treatment of hepatocellular carcinoma: results of the PRECISION V study, *Cardiovasc. Intervent. Radiol.* 33 (2010) 41–52.
- [15] M. Varela, M.I. Real, M. Burrel, A. Forner, M. Sala, M. Brunet, C. Ayuso, L. Castells, X. Montana, J.M. Llovet, J. Bruix, Chemoembolization of hepatocellular carcinoma with drug eluting beads: efficacy and doxorubicin pharmacokinetics, *J. Hepatol.* 46 (2007) 474.
- [16] L.J. Waters, T.S. Swaine, A.L. Lewis, A calorimetric investigation of doxorubicin-polymer bead interactions, *Int. J. Pharm.* 493 (2015) 129–133.
- [17] T. de Baere, S. Plotkin, R. Yu, A. Sutter, Y. Wu, G.M. Cruise, An in vitro evaluation of four types of drug-eluting microspheres loaded with doxorubicin, *J. Vasc. Interv. Radiol.* 27 (2016) 1425–1431.
- [18] P.L. Pereira, S. Plotkin, R. Yu, A. Sutter, Y. Wu, C.M. Sommer, G.M. Cruise, An in vitro evaluation of three types of drug-eluting microspheres loaded with irinotecan, *Anticancer Drugs* 27 (2016) 873–878.
- [19] C.L. Heaysman, Structure-Property Relationships of Charged Copolymer Microspheres for Drug Delivery [PhD Thesis], University of Brighton, 2009.
- [20] M. Keese, L. Gasimova, K. Schwenke, V. Yagublu, E. Shang, R. Faissner, A. Lewis, S. Samel, M. Lohr, Doxorubicin and mitoxantrone drug eluting beads for the treatment of experimental peritoneal carcinomatosis in colorectal cancer, *Int. J. Cancer* 124 (2009) 2701–2708.
- [21] A.L. Lewis, DC Bead<sup>™</sup>: a major development in the toolbox for the interventional oncologist, *Expert Rev. Med. Devices* 6 (2009) 389–400.
- [22] C.L. Heaysman, G.J. Phillips, A.W. Lloyd, A.L. Lewis, Synthesis and characterisation of cationic quaternary ammonium-modified polyvinyl alcohol hydrogel beads as a drug delivery embolisation system, *J. Mater. Sci. – Mater. Med.* 27 (2016) 53–62.
- [23] N.V. Bhat, M.M. Nate, M.B. Kurup, V.A. Bambole, S. Sabharwal, Effect of  $\gamma$ -radiation on the structure and morphology of polyvinyl alcohol films, *Nucl. Instrum. Methods Phys. Res. B* 237 (2005) 585–592.
- [24] R.M. Silverstein, F.X. Webster, D.J. Kiemle, Chapter 2 infrared spectrometry, in: *Spectrometric Identification of Organic Compounds*, 7th ed., John Wiley & Sons, Inc., Hoboken, N.J., 2005.
- [25] C.A. Finch, *Polyvinyl Alcohol: Properties and Applications*, John Wiley & Sons, Bristol, 1973.
- [26] W. Kemp, *Organic Spectroscopy*, Hong Kong: Macmillan Publishers Ltd, London, 1984.
- [27] M.V. Gonzalez Fajardo, Delivery of Drugs from Embolisation Microspheres [PhD Thesis], University of Brighton, 2006.
- [28] O. Demchenko, N. Kutsevol, T. Zheltonozhskaya, V. Syromyatnikov, About the compatibility of polymer components in polymer complexes based on poly (acrylamide) and poly(vinyl alcohol), *Macromolecular Symposia* 166 (2001) 117–122.
- [29] R. Arshady, Chapter 3: Definitions, Nomenclature and Terminology, in: R. Arshady (Ed.), *Microspheres Microcapsules & Liposomes*, Citus Books, London, 1999, pp. 55–81.
- [30] Y. Nagai, L.D. Unsworth, S. Koutsopoulos, S. Zhang, Slow release of molecules in self-assembling peptide nanofiber scaffold, *J. Control. Release* 115 (2006) 18–25.
- [31] S.H. Kim, W.K. Son, Y.J. Kim, E.G. Kang, D.W. Kim, C.W. Park, W.-G. Kim, H.-J. Kim, Synthesis of polystyrene/poly(butyl acrylate) core-shell latex and its surface morphology, *J. Appl. Polym. Sci.* 88 (2003) 595–601.
- [32] J.H. Yeum, Q.S.Y. Deng, Poly(vinyl acetate)/silver nanocomposite microspheres prepared by suspension polymerization at low temperature, *Macromol. Mater. Eng.* 290 (2005) 78–84.
- [33] N. Konishi, T. Fujibayashi, T. Tanaka, H. Minami, M. Okubo, Effects of properties of the surface layer of seed particles on the formation of golf ball-like polymer particles by seeded dispersion polymerization, *Polym. J.* 42 (2010) 66–71.
- [34] M. Dai, L. Song, W. Nie, Y. Zhou, Golf ball-like particles fabricated by nonsolvent/solvent-induced phase separation method, *J. Colloid Interface Sci.* 391 (2013) 168–171.
- [35] J.-H. Lee, C.-S. Lee, K.-Y. Cho, Enhanced cell adhesion to the dimpled surfaces of golf-ball-shaped microparticles, *ACS Appl. Mater. Interfaces* 6 (2014) 16493–16497.
- [36] F. Mohamed, C.F. van der Walle, PLGA microcapsules with novel dimpled surfaces for pulmonary delivery of DNA, *Int. J. Pharm.* 311 (2006) 97–107.